LAWRENCE
LIVERMORE
NATIONAL
LABORATORY

LLNL-JRNL-423077

Monitoring annealing via carbon dioxide laser heating of defect populations in fused silica surfaces using photoluminescence microscopy

R.N. Raman, M.J. Matthews, J.J. Adams, S.G. Demos

February 2, 2010

Monitoring annealing via carbon dioxide laser heating of defect populations in fused silica surfaces using photoluminescence microscopy

Disclaimer

Monitoring annealing via CO_2 laser heating of defect populations in fused silica surfaces using photoluminescence microscopy

Rajesh N. Raman*, Manyalibo J. Matthews, John J. Adams, and Stavros G. Demos
Lawrence Livermore National Laboratory, 7000 East Ave, Livermore, CA, USA 94551

ABSTRACT

Photoluminescence microscopy and spectroscopy under 266 nm and 355 nm laser excitation are explored as a means of monitoring defect populations in laser-modified sites on the surface of fused silica and their subsequent response to heating to different temperatures via exposure to a CO_2 laser beam. The results indicate that the defect concentrations decrease significantly with increasing CO_2 laser exposure and are nearly eliminated when the peak surface temperature exceeds the softening point of fused silica (~1900K), suggesting that this method might be suitable for *in situ* monitoring of repair of defective sites in fused silica optical components.

Keywords: photoluminescence microscopy, fused silica, surface defects, oxygen-deficiency centers, non-bridging oxygen hole centers, laser-induced defects, CO_2 laser

Fused silica is commonly used for the manufacturing of optical elements for high average laser power applications such as microlithography, deep UV and excimer lasers, and large aperture laser systems designed to achieve laser-driven inertial confinement fusion (ICF). The large photon energies used in these applications result in degradation of material performance mainly via generation of atomic defects or the formation of macroscopically observed damage sites, thus limiting system performance and increasing cost of operation. Exposure of fused silica to temperatures and pressures created during a laser-induced damage event [1] causes material modifications which include the formation of a crater, creation of micro-fractures, and the generation of a number of defects [2-7]. Studies have shown that upon damage initiation on the surface of optical components for ICF class laser systems, subsequent laser pulses can grow these damage sites to macroscopic dimensions [8-9]. To avoid having to replace the optic each time a damage event occurs, extensive research has been directed towards increasing the lifetime of these optics by arresting damage site growth [10-11]. One of the most promising methods towards this goal involves exposure of the damage site to a CO_2 laser [12], thereby increasing the local temperature to the point where cracks can be fused together. The development of *in situ* diagnostic tools [3,7,13] to guide this repair process requires a better understanding of the processes involved, including thermally-activated annihilation of the absorbing defects that have been postulated to play a key role in the re-initiation of the damage process at pre-existing damage sites leading to damage growth [3,4,7,14-16].

Photoluminescence (PL) microscopy has the potential to offer such diagnostic capabilities because it can spatially map the concentration of various defect species in laser-modified fused silica, namely oxygen deficiency centers (ODC), unknown laser-induced defects (referred to as LID), and non-bridging oxygen hole centers (NBOHC), which are known to have specific PL emission bands centered at ~470, 560, and 650 nm, respectively [2,3-4,17]. In this work we evaluate PL microscopy under UV excitation as a means of monitoring the distribution of defects formed following laser damage and over various CO_2 laser treatments (corresponding to various surface temperatures). The objective of this work is two-fold: 1) to develop a better understanding of the annihilation efficiency of the different defect species as a function of the surface temperature and 2) to develop a tool that can be used as an *in situ* diagnostic during the implementation of various repair protocols.

Experiments were conducted on a 5 cm-diameter, 1 cm-thick Corning 7980 fused silica sample. Fifty-eight damage sites were formed on the exit surface of the sample in a grid pattern with site nearest-neighbor separation of 3 mm. Each damage site was initiated by a single 7-ns FWHM pulse from a Nd:YAG laser operating at 355 nm with a fluence at the exit surface of the sample of ~30 J/cm^2. These sites were then grown simultaneously on the exit surface using a sequence of 5-ns, flat-in-time pulses with an average fluence of ~10 J/cm^2 at 351 nm delivered in a spatially uniform, large area laser beam [18].

Thirty of the 58 damage sites were subsequently exposed for 40 s to different irradiances from a CO_2 laser operating at 10.6 μm wavelength and with a 1/e beam radius of a=0.71 mm. These 30 sites were then categorized into 6 sets (5 sites per set) corresponding to 6 levels of CO_2 laser peak axial irradiance: I=0.44, 0.57, 0.63, 0.69, 0.76 and 0.88 kW/cm^2. A thermal imaging system described in detail in Ref. 19 was utilized to estimate the surface temperature profile under these exposure conditions to the CO_2 laser. In that study, it was shown that the peak steady-state temperature rise can be reasonably estimated by $\Delta T \sim \sqrt{\pi a} I_a / 2k$, where I_a is the absorbed irradiance (which takes into account the 15% reflectivity of silica at 10.6 μm) and k=0.020W/cm·K. Hence, the corresponding surface temperatures are approximated as 1500, 1800, 2000, 2200, 2300, and 2700 K, respectively, for the irradiances listed above. The remaining damage sites (n=28) received no CO_2 laser exposure and served as control sites.

For the purpose of monitoring the distribution of defects in damage sites as a function of increasing CO_2 laser exposure, we employed a portable PL microscopy system [20] consisting of a long working-distance, 5X magnification objective (Mitutoyo, Japan) and a 5X zoom lens, followed by a 420 nm long-pass filter. To eliminate the possibility of photobleaching, the excitation was provided by two low-irradiance (3 mW/cm^2) compact laser sources operating at 266 nm and 355 nm wavelengths. Images were captured using a liquid nitrogen-cooled CCD (1340 x 1300 pixels) under either excitation with integration times ranging from 30-180 s. Ring-illuminated white light scattering (LS) images of the same sites were also recorded. The spatial resolution for both the PL and LS images was on the order of 2 μm.

PL spectra were first acquired from the control damage sites. Typical spectra are shown in Fig. 1. The labels A and B refer to two different locations from within the same damage site. The spectra under 266 nm excitation contain one prominent emission peak centered at ~470 nm (corresponding to ODC) and a weaker peak at ~650 nm (minor contribution from NBOHC). In contrast, the spectra under 355 nm excitation contain two emission peaks, one centered at ~560 nm (corresponding to LID defects, see Ref. 4) and the other at ~650 nm (corresponding to NBOHC). The difference in the relative intensities of these peaks at locations A and B suggests a non-uniform distribution of the same defects within a damage site.

Figure 2 displays PL (rows 1 and 2) and LS (row 3) images of selected damage sites of similar post-damage diameter (160-180 μm) after exposure to various levels of CO_2 laser irradiance, as indicated at the top of each column (one site per column). The site shown in the first column did not undergo any CO_2 laser exposure. Following the PL peak assignments described above, the image under 266 nm excitation (Fig. 2a) portrays the spatial distribution of mainly ODC defects while that under 355 nm excitation (Fig. 2e) portrays that of NBOHC and LID defects. As a result, images of the same damage site exhibit different intensity maps. However, after exposing a site to at least I=0.44 kW/cm^2 of CO_2 laser irradiance, (e.g. Figs. 2b and 2g), the differences in the resulting images under either UV excitation source virtually disappear.

The mean PL intensity of a damage site was calculated by defining a square region of interest inscribed within the region giving rise to PL in the image. The mean intensity (counts per pixel) was then calculated, and this value was normalized to the image integration time. The result of these calculations is summarized in Fig. 3, where the mean intensity is plotted as a function of the local peak surface temperature corresponding to each CO_2 laser exposure used in this study. Error bars indicate one standard deviation (n=5 sites). While the mean PL intensity from the site decreased under both excitations after I=0.44 kW/cm^2 of irradiation, the decrease under 266 nm excitation is much larger (by a factor of about 4), indicating a significant decrease in the concentration of ODC defects. It is worth noting that this exposure raises the sample surface temperature just above the glass transition temperature (T_G=1315 K) but is well below the softening point (1860 K), implying that structural relaxation over a <100 s time scale is possible but viscous flow is unlikely. The difference in the response of the PL intensity under 266 nm excitation as T_G is exceeded suggests that annihilation of ODC is thermally-activated at this temperature (1500 K) for a 40 s exposure. However, though not explicitly explored here, it could be expected that lower temperatures over longer time scales would lead to similar defect annihilation levels [21].

Mean PL intensity further decreased by a factor of about 20, but proportionally between the two excitation wavelengths, as CO_2 laser irradiance was increased to I=0.69 kW/cm^2 (corresponding to 2200 K). This result suggests that, when exceeding the softening point of fused silica (~1900 K) over a 40 s time scale, the material has sufficient thermal energy to anneal defects of all three types within the damage site through either surface diffusion or capillary action. CO_2 laser heating may facilitate the reconstruction of bonds, thus restoring the original molecular network and annihilating defects initially formed during the thermal shock [1] induced by the damage laser pulse. In addition, it has been observed that the onset of capillary-driven surface relaxation of sub-micron features on silica

surfaces using CO_2 laser exposures takes place at temperatures of ~1800 K, with complete relaxation at ~2000 K, over similar time scales [22]. Furthermore, when comparing the ring-illuminated images of Figs. 2k-2o with the PL images, the two appeared to be strongly correlated spatially. Since scattered light is enhanced from regions containing rougher surfaces, these observations suggest that material flow of roughened surfaces and annihilation of surface defects created during the initial damage event are both driven by capillary action at near-softening temperatures. A negligible amount of PL intensity above the noise level was detected from sites exposed to I=0.88 kW/cm^2, corresponding to a surface temperature of about 2700 K which is above the fused silica boiling point (2500 K). Thus, at this temperature, the majority of defective silica is expected to have been removed through evaporation.

Acknowledgments

The authors wish to thank Mary A. Norton and Gabriel M. Guss for assistance with sample preparation. This work was performed under the auspices of the U.S. Department of Energy by Lawrence Livermore National Laboratory under Contract DE-AC52-07NA27344.

References

[1] C. W. Carr, H. B. Radousky, A. M. Rubenchik, M. D. Feit, and S. G. Demos, "Localized Dynamics during Laser-Induced Damage in Optical Materials," *Phys. Rev. Lett.* **92**(8), 087401-1-4 (2004).

[2] L. Skuja, "The nature of optically active oxygen-deficiency-related centers in amorphous silicon dioxide," *J. Non-Cryst. Solids* **239**, 16-48 (1998).

[3] S. G. Demos, M. Staggs, K. Minoshima, and J. Fujimoto, "Characterization of laser induced damage sites in optical components," *Opt. Express* **10**(25), 1444-1450 (2002).

[4] S. O. Kucheyev and S. G. Demos, "Optical defects produced in fused silica during laser-induced breakdown," *Appl. Phys. Lett.* **82**(19), 3230-3232 (2003).

[5] J. Wong, J. L. Ferriera, E. F. Lindsey, D. L. Haupt, I. D. Hutcheon, and J. H. Kinney, "Morphology and microstructure in fused silica induced by high fluence ultraviolet 3ω (355 nm) laser pulses," *J. Non-Cryst. Solids* **352**(3), 255-272 (2006).

[6] S. Xu, X. Zu, X. Jiang, X. Yuan, J. Huang, H. Wang, Haibin Lv, and W. Zheng, "The damage mechanisms of fused silica irradiated by 355 nm laser in vacuum," *Nucl. Instrum. Meth. B* **266,** 2936–2940 (2008).

[7] T. A. Laurence, J. D. Bude, N. Shen, T. Feldman, P. E. Miller, W. A. Steele, and T. Suratwala, "Metallic-like photoluminescence and absorption in fused silica surface flaws," *Appl. Phys. Let.* **94**, 151114 (2009).

[8] M. A. Norton, L. W. Hrubresh, Z. L. Wu, E. E. Donohue, M. D. Feit, M. R. Kozlowski, D. Milam, K. P. Neeb, W. A. Molander, A. M. Rubenchik, W. D. Sell, and P. Wegner, "Growth of laser initiated damage in fused silica at 351 nm," *Proc. SPIE* **4347**, 468-468 (2001).

[9] W. Huang, W. Han, F. Wang, Y. Xiang, F. Li, B. Feng, F. Jing, X. Wei, W. Zheng, and X. Zhang, "Laser-Induced Damage Growth on Larger-Aperture Fused Silica Optical Components at 351nm," *Chin. Phys. Lett.* **26**(1) 017901 (2009).

[10] R. A. House, J. R. Bettis, and A. H. Guenther, "Efficacy of ion polishing optical surfaces," *Appl. Opt.* **16**, 1486–1488 (1977).

[11] T. Kamimura, K. Nakai, M. Yoshimura, Y. Mori, T. Sasaki, M. Tanaka, Y. Okada, H. Yoshida, M. Nakatsuka, T. Kojima, and K. Yoshida, "High damage resistivity of optical surface for UV lasers by ion beam etching," *Rev. Laser Eng.* **27**, 623–627 (1999).

[12] R. M. Brusasco, B. M. Penetrante, J. A. Butler, and L.W. Hrubesh, "Localized CO_2 laser treatment for mitigation of 351 nm damage growth on fused silica," *Proc. SPIE* **4679**, 40-47 (2002).

[13] J. Neauport, P. Cormont, P. Legros, C. Ambard, and J. Destribats, "Imaging subsurface damage of grinded fused silica optics by confocal fluorescence microscopy," *Opt. Express* **17**, 3543-3554 (2009).

[14] V. Uhl, K. O. Greulich, and S. Thomas, "Comparison of the influence of the fictive and the annealing temperature on the UV-transmission properties of synthetic fused silica," *Appl. Phys. A-Mater.* **65**, 457-462 **(**1997).

[15] C. Muhlig, W. Triebel, S. Bark-Zollmann, and D. Grebner, "In situ diagnostics of pulse laser-induced defects in DUV transparent fused silica glasses," *Nucl. Instrum. Meth. B* **166,** 698-703 (2000).

[16] R. A. Negres, M. W. Burke, P. P. DeMange, S. B. Sutton,, M. D. Feit, S. G. Demos, "Evaluation of UV absorption coefficient in laser-modified fused silica," *Appl. Phys. Lett.* **90**, 061115 (2007).

[17] P. Barritault, P. R. Bouchut, H. Bercegol, P. Chaton, and G. Ravel, "Fluorescence of mitigated laser damage in fused silica," *Proc. SPIE* **5647**, 188 (2005).

[18] R. A. Negres, M. A. Norton, Z. M. Liao, D. A. Cross, J. D. Bude and C. W. Carr, "The effect of pulse duration on the growth rate of laser-induced damage sites at 351 nm on fused silica surfaces," *Proc. SPIE* **7504**, 750412 (2010).
[19] S. T. Yang, M. J. Matthews, S. Elhadj, V. G. Draggoo, and S. E. Bisson, "Thermal transport in CO_2 laser irradiated fused silica: *In situ* measurements and analysis," *J. Appl. Phys.* **106,** 103106 (2009).
[20] S. G. Demos, C. A. Lieber, B. Lin, and R. Ramsamooj, "Imaging of tissue microstructure using a multimodal microscope design," *IEEE J. Sel. Top. Quantum Electron.* **11**, 752–758 (2005).
[21] F. Messina and M. Cannas, "Temperature dependence of the generation and decay of E' centers induced in silica by 4.7 eV laser radiation," *J. Non-Cryst. Solids* **355**, 1038-1041 (2009).
[22] N. Shen, M. J. Matthews, J. E. Fair, J. A. Britten, H. T. Nguyen, D. Cooke, S. Elhadj, and S. T. Yang, *Appl. Surf. Sci.,* submitted.

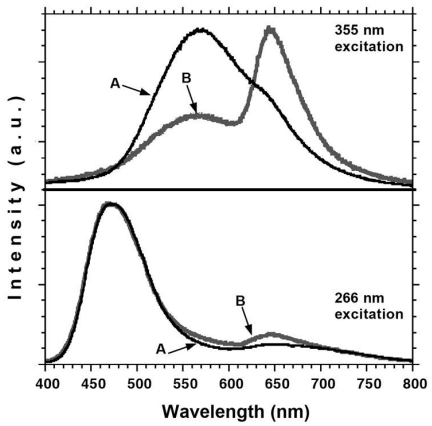

Figure 1: a) Photoluminescence spectra under UV excitation from a control damage site (without CO_2 laser exposure). Here A and B denote two different locations within the same damage site.

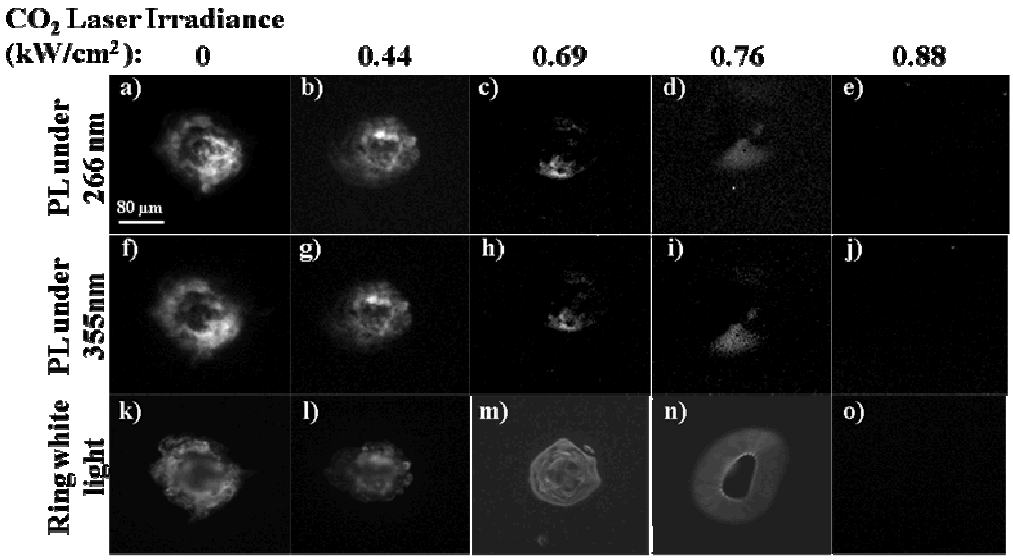

Figure 2: Images of different damage sites of similar post-damage diameter (160-180 μm) after 40-s exposure to various CO_2 laser irradiances (shown at the top of each column). Image series (a)-(e) correspond to 266 nm excitation, (f)-(j) to 355 nm excitation, and (k)-(o) to ring-illuminated white light scattering.

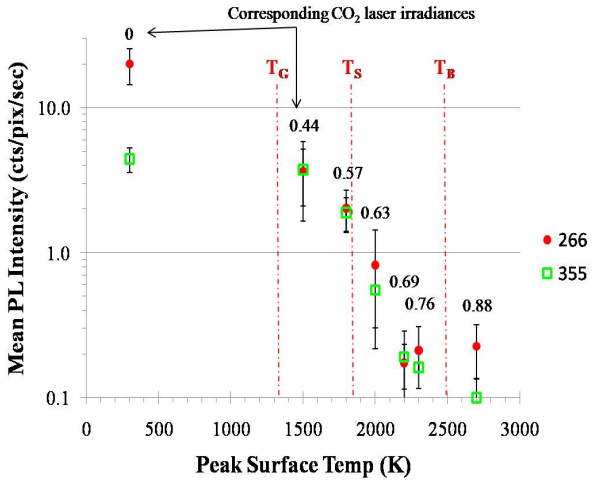

Figure 3: Mean PL intensity as a function of peak surface temperature resulting from exposure to various CO_2 laser irradiances, as labeled above each pair of data points. For reference, vertical dash-dotted lines indicate the glass transition temperature (T_G), softening point (T_S), and boiling point (T_B) of amorphous fused silica, respectively.